Pressure-induced structural transition and low-temperature recovery of sodium pentazolate

Zitong Zhao(赵梓彤), Ran Liu(刘然), Linlin Guo(郭琳琳), Shuang Liu(刘爽), Minghong Sui(隋明宏), Bo Liu(刘波), Zhen Yao(姚震)†, Peng Wang(王鹏)‡, and Bingbing Liu(刘冰冰)

State Key Laboratory of Superhard Materials, College of Physics, Jilin University, Changchun 130012, *China*

(Received 15 November 2022; revised manuscript received 2 February 2023; accepted manuscript online 6 February 2023)

Pentazolate compounds have attracted extensive attention as high energy density materials. The synthesis and recovery of pentazolate compounds is of great importance for their potential applications. Here, we report the synthesis of $Pmn2_1$-NaN_5 and Pm-Na_2N_5 through compressing and laser heating pure NaN_3 at $\sim$ 60 GPa. Upon decompression, the pressure-induced structural transition from $Pmn2_1$-NaN_5 into Cm-NaN_5 is observed in the pressure range of 14–23 GPa for the first time. The cyclo-N_5^- can be traced down to 4.7 GPa at room temperature and recovered to ambient pressure under low temperature condition (up to 160 K). The Pm-Na_2N_5 is suggested to decompose into the $P4/mmm$-NaN_2 at 23 GPa, and be stable at ambient conditions. This work provides insight into the high-pressure behaviors of pentazolate compounds and an alternative way to stabilize energetic polynitrogen compounds.

Keywords: sodium pentazolate, high pressure, laser heating, structural transition

PACS: 62.50.–p, 64.60.–i, 61.66.Fn **DOI:** 10.1088/1674-1056/acb917

1. Introduction

Pentazolate anion (cyclo-N_5^-) is a promising energetic polynitrogen specie because of the enormous energy released upon transition from cyclo-N_5^- to N_2 molecules.[1,2] Different from the other polynitrogen species, cyclo-N_5^- presents aromaticity, which provides good thermal stability to this energetic all-nitrogen five-membered ring structure.[3] Due to the high energy density and high stability, pentazolate compounds have been recognized as a new generation of high energy density materials (HEDMs) and their synthesis has been actively pursued. Success has been firstly achieved in the synthesis of a complex $(N_5)_6(H_3O)_3(NH_4)_4Cl$ and a number of metal pentazolate hydrates through traditional chemical techniques.[4–9] By using abundant coordinated water molecules, cyclo-N_5^- can be stabilized under ambient conditions through hydrogen-bonding interactions. Cyclo-N_5^- can also be stabilized only by ionic interactions, and some water-free pentazolate frameworks have been generated in recent years.[10,11]

Theoretical works revealed the formation of simple binary pentazolate compounds with much higher content of cyclo-N_5^- by introducing metal elements (e.g., Li, Na, K, Rb, Cs, Be, Mg, Ca, Sr, Ba, Al, Ga, Sc, Y, Cu, Ag, Zn) into the nitrogen system under high-pressure conditions, which indicated that the high-pressure strategy is an alternative route.[1–3,12–24] The synthesis and recovery of simple binary pentazolate compounds are important for their practical applications as HEDMs. Up to now, through high-pressure synthetic techniques, three kinds of simple binary alkali metal pentazolate compounds, such as Li-N_5, Na-N_5 and Cs-N_5, have been successfully synthesized.[3,25–27]

It is interesting that the different sodium pentazolate compounds have been obtained with the variation of precursor under similar synthesis conditions. Pm-Na_2N_5, $Pmn2_1$-NaN_5 and $P2_1/n$-$NaN_5{\cdot}N_2$ have been synthesized through compressing and laser heating pure NaN_3 and the mixture of NaN_3 and molecular N_2 respectively at $\sim$ 50 GPa.[27] These sodium pentazolate compounds are unstable below 12 GPa.[27] Theoretical works also predicted that cyclo-N_5^- can be stabilized in Cm-NaN_5 (above 20 GPa), which trends to transform into $P2/c$-NaN_5 at ambient pressure.[1] Up to now, the pressure-induced structural transition between NaN_5 in different crystal structures has not been observed and the recovery route of NaN_5 to ambient pressure is still problematic. As one of the basic thermodynamic parameters, temperature can also effectively modulate the stability of the final products as revealed in the high-pressure studies of nitrogen.[28] Thus, investigating the sodium pentazolate compounds in a wider temperature range is necessary.

In this work, we synthesized the $Pmn2_1$-NaN_5 and Pm-Na_2N_5 by directly compressing and laser heating NaN_3 at $\sim$ 60 GPa and characterized the products by using *in situ* XRD and Raman measurements. Upon decompression, the $Pmn2_1$-NaN_5 compound undergoes a structural transition into Cm-NaN_5 in the pressure range of 14–23 GPa. And the pressure-produced cyclo-N_5^- can be traced down to 4.7 GPa. The Pm-Na_2N_5 compound is suggested to decompose into the $P4/mmm$-NaN_2 at 23 GPa, and the NaN_2 compound can be traced down to ambient conditions. The low temperature experiment indicates that the cyclo-N_5^- can be recovered at ambient pressure up to 160 K.

†Corresponding author. E-mail: yaozhen@jlu.edu.cn
‡Corresponding author. E-mail: wangpengtrrs@jlu.edu.cn

© 2023 Chinese Physical Society and IOP Publishing Ltd

2. Materials and methods

NaN_3 (CAS: 26628-22-8, β-NaN_3) was purchased from AMERSCO Inc. and used as the precursor material. The diamond anvil cell (DAC) with 300 μm diameter culets was used to perform high-pressure experiments. The NaN_3 sample was firstly loaded between two pieces of dried NaCl (sandwich structure) in the sample chamber in a glove box filled with argon gas, and then compressed up to 60 GPa. NaCl pieces were used as thermal insulating layers. The pressures were calibrated by both the R1-line emission of a tiny ruby ball and the sharp high-frequency edge of the diamond anvil.[29–31] A laser beam (λ = 1064 nm) was used to heat the NaN_3 sample to ~ 2000 K. The temperature, calibrated by blackbody radiation, was collected by a spectrometer (Princeton Instruments, Acton SP-2360) with a InGaAs CCD detector (Princeton Instruments, PyLon-IR: 1024). *In situ* high-pressure Raman spectral measurements were performed by a Raman spectrometer (Horiba Jobin-Yvon, LabRAM HR Evolution) excited by a 473 nm laser. And a customized cryostat (Cryo Industries of America, Inc) with liquid nitrogen as the cryogen was used to achieve low-temperature conditions. *In situ* high-pressure XRD measurements were carried out at the BL15U1 beam line of Shanghai Synchrotron Radiation Facility (SSRF) (λ = 0.6199 Å). The diffraction data were collected by a MAR CCD detector. The sample-to-detector distance and the image plate orientation angles were calibrated by the CeO_2 standard. The two-dimensional XRD images were analyzed with the Dioptas software, and the obtained XRD patterns were refined by using the GSAS software package with the Le Bail method.

Theoretical calculations of geometry optimization and formation enthalpy were based on the first-principles density functional theory (DFT) method performed with the Vienna *ab initio* simulation (VASP) package. The generalized gradient approximation (GGA) with Perdew–Burke–Ernzerhof (PBE) was used to describe the exchange correlation energy. The convergence criteria of atomic force and electronic self-consistent energy were set to 1 meV/Å and 1×10^{-5} eV, respectively. To ensure the energy calculations converged, we set the energy cutoff at 520 eV and a *k*-mesh spacing at $2\pi \times 0.03$ Å^{-1} for Brillouin zone sampling. The Raman and IR spectra were obtained by the CASTEP code in the Materials Studio package. The norm-conserving pseudopotentials were used to describe the ionic potentials. The convergence criteria of atomic force and electronic self-consistent energy were set to 0.05 eV/Å and 2×10^{-5} eV, respectively.

3. Results and discussion

At around 60 GPa, the laser-heated NaN_3 sample transformed into novel Na–N compounds, which were identified by the XRD pattern and the Raman spectrum as shown in Figs. 1 and 2. We firstly performed Le Bail refinement of the experimental XRD pattern at 60 GPa with the structural modes of *Pm*-Na_2N_5 and NaCl-B2, as shown in Fig. S1.[27] The refinement result indicates that only *Pm*-Na_2N_5 structure cannot well match the experimental XRD pattern of new-formed Na–N compound. The XRD pattern obtained from the laser-heated sample at 60 GPa has been compared with the simulated XRD patterns of the *Pmn*2$_1$-NaN_5, *Pm*-Na_2N_5 and *Cmmm*-NaN_2 structures, which were predicted to be stable at 60 GPa, as shown in Fig. S2.[1,27] It is evident that the mixture of the simulated XRD patterns can match with the experimental XRD pattern. To further confirm the new-formed Na–N compounds, the relative enthalpy differences between *I*4/*mcm*-NaN_3 structure and structures of different chemical transition products have been calculated, as shown in Fig. S3, demonstrating that the mixture of *Pmn*2$_1$-NaN_5 and *Pm*-Na_2N_5 is energetically preferred above 30 GPa.[1,27,32] Le Bail refinement of the experimental XRD pattern is shown in Fig. 1(a). The *Pmn*2$_1$-NaN_5 crystallizes in the orthorhombic unit cell with lattice parameters $a = 5.391(3)$ Å, $b = 2.825(8)$ Å and $c = 5.804(4)$ Å at 60 GPa (see Table S1). In the *Pmn*2$_1$-NaN_5 structure, planar N_5^- rings stack along the *b*-axis, and each Na atom is coordinated with seven N_5^- rings, as shown in Figs. S4(a) and S4(c). And the *Pm*-Na_2N_5crystallizes in the monoclinic unit cell with $a = 4.765(0)$ Å, $b = 2.517(1)$ Å, $c = 4.852(1)$ Å and $\beta = 118.64(0)^\circ$ at 60 GPa (see Table S1). In the *Pm*-Na_2N_5 structure, planar N_5^- rings stack along the *b*-axis, and each Na atom is coordinated with six N_5^- rings.[27] Different from the previous work,[27] in this study, under higher pressure condition of ~ 60 GPa, sodium pentazolate is obtained through a chemical route suggested as $5NaN_3 \rightarrow NaN_5 + 2Na_2N_5$.

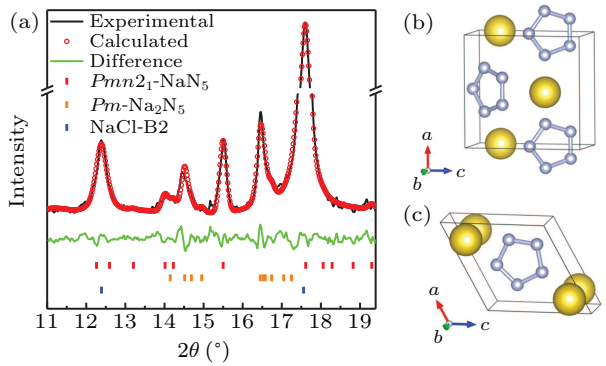


Fig. 1. (a) Le Bail refinement of the XRD pattern obtained from the laser-heated NaN_3 sample at 60 GPa. (b) The crystal structures of *Pmn*2$_1$-NaN_5 and (c) *Pm*-Na_2N_5 at 60 GPa (the yellow and gray spheres represent the Na and N atoms, respectively).

Raman spectra of NaN_3 before and after laser heating at 60.5 GPa are shown in Fig. S5. Compared with the Raman spectrum of unheated NaN_3, it is evident that the intense symmetric stretching mode of N_3^- around 1513 cm^{-1} (marked with black points) cannot be observed after laser heating, indicating the disappearance of NaN_3. Furthermore, a series of new broad bands emerge around 257 cm^{-1}, 479 cm^{-1}, 878 cm^{-1},

1036 cm^{-1} and 1207 cm^{-1}, which cannot be attributed to NaN_3, indicating the formation of new Na–N compounds.

According to the XRD results, we performed the theoretical calculations of the Raman-active modes of *Pmn*2$_1$-NaN_5 and *Pm*-Na_2N_5 at 60 GPa, as shown in Fig. 2. The low-frequency Raman bands (257–479 cm^{-1}) can be assigned to the lattice vibration modes of *Pm*-Na_2N_5, and lattice vibration modes of *Pmn*2$_1$-NaN_5 are difficult to be distinguished from those of *Pm*-Na_2N_5 because of the broad linewidths.[27] The high-frequency Raman bands (1036–1207 cm^{-1}) are related with the in-plane stretching modes of N_5 rings in *Pmn*2$_1$-NaN_5 and *Pm*-Na_2N_5. There is also a Raman band centered at $\sim$ 878 cm^{-1} close to the predicted bending mode of N_5^- anion in *Pmn*2$_1$-NaN_5. The most intense N_5^- breathing mode with simulated wavenumber of 1275 cm^{-1} is suggested to be screened by the intense first-order Raman peak of diamond at 60.5 GPa, considering the evolution of Raman spectra upon decompression (see Fig. 5(a)). Our Raman spectrum provides further confirmation about the formation of *Pmn*2$_1$-NaN_5 and *Pm*-Na_2N_5.

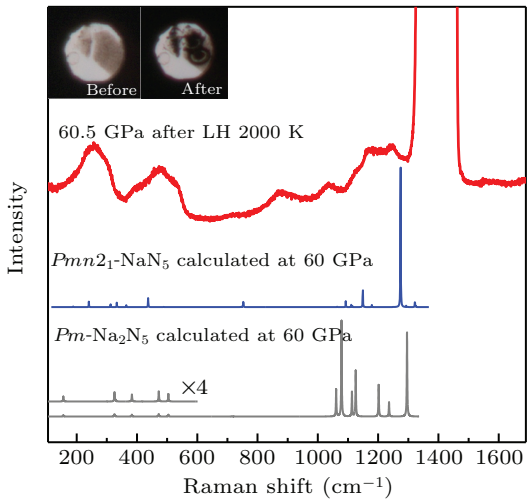


Fig. 2. Experimental Raman spectrum of the laser-heated sample at 60.5 GPa (red curve) compared with theoretical Raman spectra of *Pmn*2$_1$-NaN_5 (blue line) and *Pm*-Na_2N_5 (gray line) at 60 GPa. And the inset shows microphotographs of the sample before (left) and after (right) laser heating, indicating the synthesis of completely opaque products.

To study the stability of sodium pentazolate compounds upon decompression, *in situ* XRD as well as Raman measurements were carried out. The corresponding XRD patterns upon decompression are shown in Fig. 3(a). With releasing pressure down to 23 GPa, all the diffraction peaks belonging to *Pmn*2$_1$-NaN_5 and *Pm*-Na_2N_5 cannot be observed, and three new diffraction peaks (marked by black dash lines) appear at 15.07°, 17.19° and 18.98°. At 14 GPa, two other new diffraction peaks appear at 13.46° and 14.74°, marked by black arrows. All these phenomena indicate the pressure-induced transitions of *Pmn*2$_1$-NaN_5 and *Pm*-Na_2N_5. Le Bail refinement against the experimental XRD pattern reveals the existence of *Cm*-NaN_5 and *P*4/*mmm*-NaN_2, as shown in Fig. 3(b).[1] The calculated enthalpy difference curves of the *Pmn*2$_1$-NaN_5 and *Cm*-NaN_5 in the pressure range of 0–60 GPa (see Fig. S6) reveals that *Cm*-NaN_5 is more energetically favorable below 23 GPa, which is in agreement with the XRD results. Thus, we can conclude that there is a structural transition from *Pmn*2$_1$-NaN_5 to *Cm*-NaN_5 occurring in the pressure range of 14–23 GPa. The *Cm*-NaN_5 has monoclinic symmetry with lattice parameters of $a = 6.063(8)$ Å, $b = 5.599(0)$ Å, $c = 3.127(3)$ Å and $\beta = 76.813(6)°$ at 14 GPa (see Table S2). In the *Cm*-NaN_5 structure, the N_5^- rings stack along the *a*-axis, and the coordination of Na atoms down to six N_5^- rings, as shown in Figs. S4(b) and S4(d). The *P*4/*mmm*-NaN_2 structure has been synthesized by laser heating NaN_3 at 4 GPa or laser heating NaN_3 with excess N_2 at 14 GPa.[27,33] While in this study, the *P*4/*mmm*-NaN_2 (see Figu. 4(b)) is suggested to be related with the chemical transition of *Pm*-Na_2N_5 at 23 GPa. Below 14 GPa, the diffraction peaks of *Cm*-NaN_5 cannot be identified. The XRD pattern at ambient condition can be indexed using *P*4/*mmm*-NaN_2 and β-NaN_3 (see Fig. S7),[1,34] indicating the possible transition from NaN_5 to NaN_3.

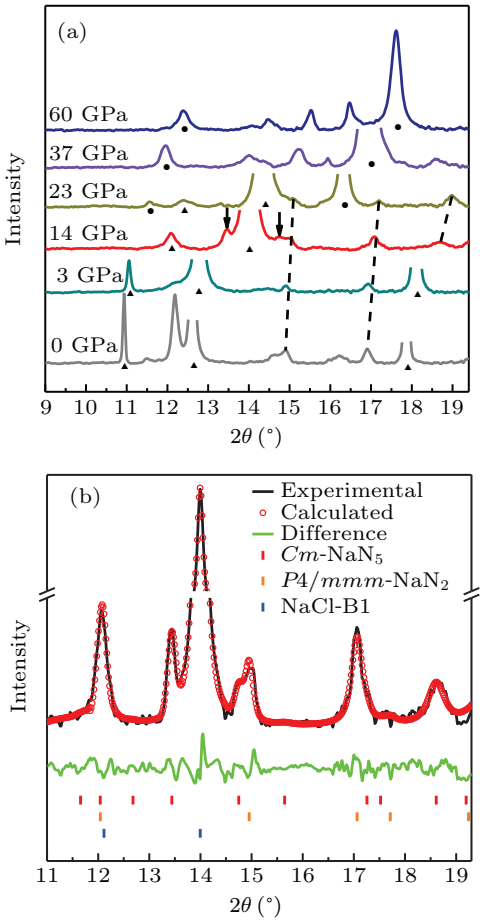


Fig. 3. (a) XRD patterns of the laser-heated sample upon decompression from 60 GPa down to ambient conditions. The black points and triangles represent the diffraction peaks of NaCl-B2/B1, respectively. The black arrows and lines represent the new diffraction peaks. (b) Le Bail refinement of the XRD pattern obtained from the laser-heated sample at 14 GPa.

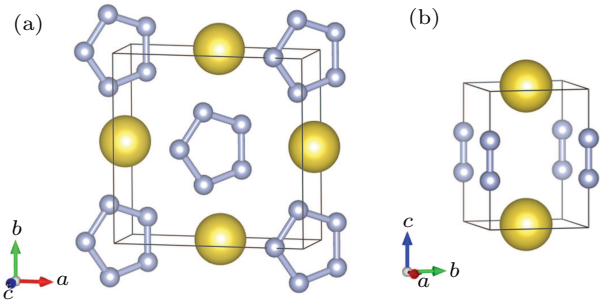


Fig. 4. The crystal structures of (a) *Cm*-NaN_5 and (b) *P*4/*mmm*-NaN_2 at 14 GPa (the yellow and gray spheres represent the Na and N atoms, respectively).

Raman spectra of the laser-heated sample upon decompression are shown in Fig. 5(a). All the characteristic Raman peaks of *Pmn*2_1-NaN_5 and *Pm*-Na_2N_5 gradually become broadened upon releasing pressure. At $\sim$ 40 GPa, the most intense breathing mode of *Pmn*2_1-NaN_5 appears from the left shoulder of intense Raman peak of diamond at $\sim$ 1300 cm^{-1}. At 17 GPa, new low-frequency vibrational peaks appear at $\sim$ 280 cm^{-1} and 380 cm^{-1}, which is consistent with the transition observed in XRD measurements in the pressure range of 14–23 GPa. According to the XRD results, we calculated the Raman-active modes of *Cm*-NaN_5, which can match with these observed Raman peaks, as shown in Fig. 5(b).[1] The low-frequency (280 cm^{-1} and 380 cm^{-1}) and high-frequency (1240 cm^{-1}) Raman peaks can be assigned to lattice and breathing modes of *Cm*-NaN_5, respectively. With further decompression, the breathing mode of *Cm*-NaN_5 can finally be traced down to 4.7 GPa. Compared with the previously reported Na–N_5 compounds, *Cm*-NaN_5 presents enhanced stability upon decompression.[27] At ambient conditions, except the intense diamond peak, the sharp Raman peaks at $\sim$ 120 cm^{-1} and 1360 cm^{-1} can be assigned to the lattice mode and symmetric stretching mode of N_3^- of β-NaN_3, respectively.[35] These results indicate that the synthesized NaN_5 in this study can be stabilized down to 4.7 GPa at room temperature and finally decomposes into NaN_3 under ambient conditions. The pressure-dependence of typical Raman peaks of the laser-heated sample has been compared with those of *Pmn*2_1-NaN_5 and *Pm*-Na_2N_5 observed in the previous study, which can reveal more accurate correlation.[27] As shown in Fig. S8, the pressure-dependence of Raman peaks in the frequency range of 100–500 cm^{-1} of the laser-heated sample can match well with those of *Pm*-Na_2N_5 in the pressure range of 20–60 GPa, and presents evident variation below 20 GPa. In the range of 900–1200 cm^{-1}, the pressure-dependence of our Raman peaks is in agreement with both *Pm*-Na_2N_5 and *Pmn*2_1-NaN_5. And the pressure-dependence of Raman peak in the frequency range of 1200–1300 cm^{-1} is in good agreement with that of the most intense N_5^- breathing mode of *Pmn*2_1-NaN_5. Thus, our Raman data further supports the existences of both *Pmn*2_1-NaN_5 and *Pm*-Na_2N_5 in the laser-heated sample.

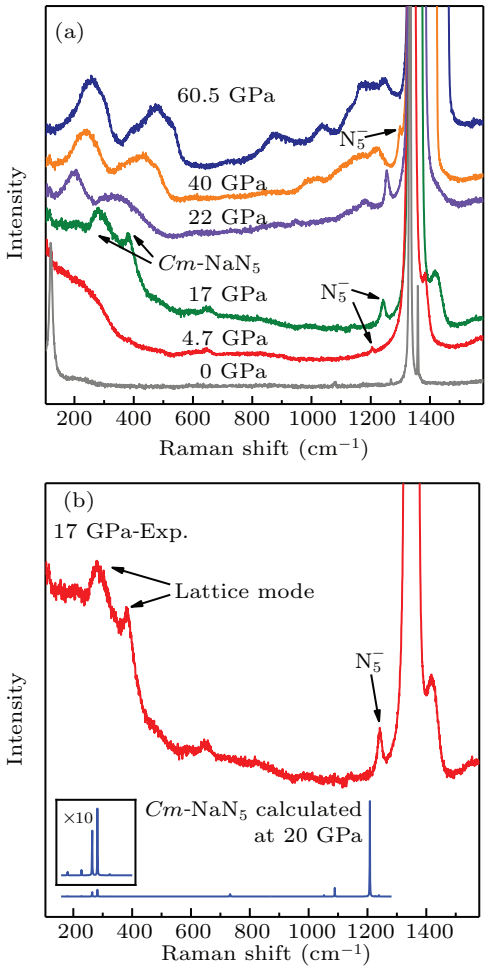


Fig. 5. (a) Experimental Raman spectra of the laser-heated sample upon decompression. (b) Experimental Raman spectrum of the laser-heated sample at 17 GPa (red curve) compared with the theoretical Raman spectrum of *Cm*-NaN_5 (blue line).

To explore the recovery route for NaN_5, decompressing Raman spectral measurements were also performed under low-temperature conditions, as shown in Fig. 6. The laser-heated sample was firstly decompressed to 37 GPa at room temperature and the most intense breathing mode of *Pmn*2_1-NaN_5 appeared on the left shoulder of the intense Raman peak of diamond at $\sim$ 1294 cm^{-1}. Then we released the pressure and decreased temperature simultaneously. At 13 GPa and 100 K, two new Raman peaks appeared at $\sim$ 280 cm^{-1} and 370 cm^{-1}, which can be assigned to the lattice vibration modes of *Cm*-NaN_5. The same structural transition from *Pmn*2_1-NaN_5 to *Cm*-NaN_5 can also be observed under low temperature condition. Moreover, a new Raman peak has been observed at 980 cm^{-1} under low-temperature conditions and cannot be attributed to the simulated Raman-active vibrational modes of *Cm*-NaN_5. According to the theoretical calculation of infrared (IR) active modes of *Cm*-NaN_5, it is suggested that this new Raman peak arises from the transition from IR activity to Raman activity of the in-plane stretching mode at

$\sim$ 1048 cm^{-1} under low-temperature and high-pressure conditions (see Fig. S9). At ambient pressure and 100 K, the most intense breathing mode of cyclo-N_5^- can still be identified at $\sim$ 1270 cm^{-1}. The pressure dependence of the typical Raman peaks of NaN_5 under low-temperature conditions is shown in Fig. S10. Comparing with the decompression process under room-temperature condition, the intense breathing mode of *Cm*-NaN_5 shifts more slowly under the low-temperature condition with releasing pressure, and the stabilities of *Pmn*2$_1$-NaN_5 and *Cm*-NaN_5 both get enhanced with the evident hysteresis in stabilization pressure (4–4.7 GPa). Then we started to warm up the sample, this breathing mode of cyclo-N_5^- can be tracked up to ambient pressure at 160 K, but eventually disappears at 220 K. Our results realize the recovery of NaN_5 with synergetic modulation of pressure and temperature, indicating an effective route to stabilize pentazolate compounds.

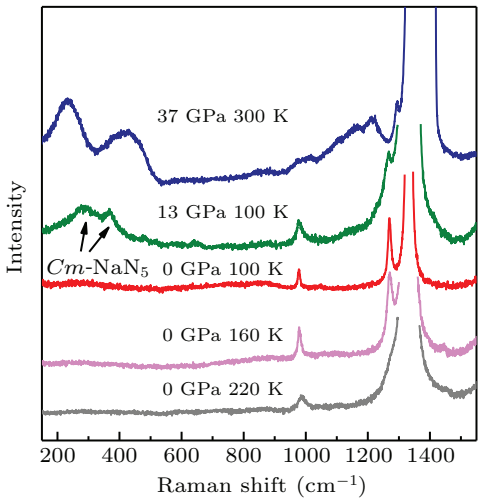


Fig. 6. Raman spectra of the laser-heated sample upon decompression from 37 GPa to ambient pressure under low-temperature conditions and during warming up process.

4. Conclusion and perspectives

To summarize, we have synthesized the *Pmn*2$_1$-NaN_5 and *Pm*-Na_2N_5 by a chemical transition of NaN_3 at $\sim$ 60 GPa accompanied by laser-heating. Upon decompression, both Raman and XRD measurements indicate the pressure-induced structural transition from *Pmn*2$_1$-NaN_5 into *Cm*-NaN_5 in the pressure range of 14–23 GPa. The chemical transition from *Pm*-Na_2N_5 into *P*4/*mmm*-NaN_2 has also been observed at 23 GPa. The cyclo-N_5^- can be traced down to 4.7 GPa at room temperature and recovered to ambient pressure at 160 K. Our work reveals the pressure-induced structural evolution of energetic NaN_5 and provides an alternative stabilization route for pentazolate compounds.

Acknowledgements

Project supported by the National Key R&D Program of China (Grant No. 2018YFA0305900), the National Natural Science Foundation of China (Grant Nos. 12174143, 11634004, 11847094, and 11804384), and JLU Science and Technology Innovative Research Team (Grant No. 2017TD-01).

References

[1] Steele B A and Oleynik I I 2016 *Chem. Phys. Lett.* **643** 21
[2] Peng F, Yao Y S, Liu H Y and Ma Y M 2015 *J. Phys. Chem. Lett.* **6** 2363
[3] Steele B A, Stavrou E, Crowhurst J C, Zaug J M, Prakapenka V B and Oleynik I I 2017 *Chem. Mater.* **29** 735
[4] Zhang C, Sun C G, Hu B C, Yu C M and Lu M 2017 *Science* **355** 374
[5] Zhang C, Yang C, Hu B C, Yu C M, Zheng Z S and Sun C G 2017 *Angew. Chem. Int. Ed.* **56** 4512
[6] Xu Y G, Wang Q, Shen C, Lin Q H, Wang P C and Lu M 2017 *Nature* **549** 78
[7] Xu Y G, Wang P C, Lin Q H and Lu M 2017 *Dalton Trans.* **46** 14088
[8] Xu Y G, Wang P C, Lin Q H, Mei X F and Lu M 2018 *Dalton Trans.* **47** 1398
[9] Li J C, Wang K C, Song S W, Qi X J, Zhang W Q, Deng M C and Zhang Q H 2019 *Sci. China Mater.* **62** 283
[10] Xu Y G, Lin Q H, Wang P C and Lu M 2018 *Chem. Asian J.* **13** 1669
[11] Zhang W Q, Wang K C, Li J C, Lin Z E, Song S W, Huang S L, Liu Y, Nie F D and Zhang Q H 2018 *Angew. Chem. Int. Ed.* **57** 2592
[12] Shen Y Q, Oganov A R, Qian G R, Zhang J, Dong H F, Zhu Q and Zhou Z X 2015 *Sci. Rep.* **5** 14204
[13] Steele B A and Oleynik I I 2017 *J. Phys. Chem. A* **121** 8955
[14] Williams A S, Steele B A and Oleynik I I 2017 *J. Chem. Phys.* **147** 234701
[15] Steele B A, Stavrous E, Prakapenka V B, Radousky H, Zaug J, Crowhurst J C and Oleynik I I 2017 *AIP Conf. Proc.* **1793** 040016
[16] Wang Z X, Yang T, Yang B C and Yi W C 2020 *CrystEngComm* **22** 6057
[17] Xia K, Zheng X X, Yuan J N, Liu C, Gao H, Wu Q and Sun J 2019 *J. Phys. Chem. C* **123** 10205
[18] Zhu S S, Peng F, Liu H Y, Majumdar A, Gao T and Yao Y S 2016 *Inorg. Chem.* **55** 7550
[19] Wei S L, Lian L L, Liu Y, Li D, Liu Z and Cui T 2020 *Phys. Chem. Chem. Phys.* **22** 5242
[20] Huang B W and Frapper G 2018 *Chem. Mater.* **30** 7623
[21] Xia K, Yuan J N, Zheng X X, Liu C, Gao H, Wu Q and Sun J 2019 *J. Phys. Chem. Lett.* **10** 6166
[22] Li J F, Sun L, Wang X L, Zhu H Y and Miao M S 2018 *J. Phys. Chem. C* **122** 22339
[23] Ding Z Y, Gao P, Lu M, Wang G X and Gong X D 2020 *J. Chin. Chem. Soc.* **67** 235
[24] Williams A S, Cong K N, Gonzalez J M and Oleynik I I 2021 *Dalton Trans.* **50** 16364
[25] Laniel D, Weck G, Gaiffe G, Garbarino G and Loubeyre P 2018 *J. Phys. Chem. Lett.* **9** 1600
[26] Zhou M, Sui M H, Shi X H, Zhao Z T, Guo L L, Liu B, Liu R, Wang P and Liu B B 2020 *J. Phys. Chem. C* **124** 11825
[27] Bykov M, Bykova E, Chariton S, Prakapenka V B, Batyrev I G, Mahmood M. F and Goncharov A F 2021 *Dalton Trans.* **50** 7229
[28] Eremets M I, Hemley R J, Mao H K and Gregoryanz E 2001 *Nature* **411** 170
[29] Mao H K, Xu J and Bell P M 1986 *J. Geophys. Res. Solid Earth* **91** 4673
[30] Hanfland M and Syassen K 1985 *J. Appl. Phys.* **57** 2752
[31] Eremets M I 2003 *J. Raman Spectrosc.* **34** 515
[32] Zhou M, Liu S J, Du M R, Shi X H, Zhao Z T, Guo L L, Liu B, Liu R, Wang P and Liu B B 2020 *J. Phys. Chem. C* **124** 19904
[33] Bykov M, Tasca K R, Batyrev I G, Smith D, Glazyrin K, Chariton S, Mahmood M and Goncharov A F 2020 *Inorg. Chem.* **59** 14819
[34] Zhu H Y, Zhang F X, Ji C, Hou D B, Wu J Z, Hannon T and Ma Y Z 2013 *J. Appl. Phys.* **113** 033511
[35] Li D M, Zhu P F, Jiang J R, Xu D, Liu R, Wang X L, Cui Q L and Zhu H Y 2017 *J. Phys. Commun.* **1** 025002